Communicated by Gordon Shepherd

A Computer Simulation of Oscillatory Behavior in Primary Visual Cortex

Matthew A. Wilson
James M. Bower
Computation and Neural Systems Program,
California Institute of Technology, Pasadena, CA 91125 USA

Periodic variations in correlated cellular activity have been observed in many regions of the cerebral cortex. The recent discovery of stimulus-dependent, spatially-coherent oscillations in primary visual cortex of the cat has led to suggestions of neural information encoding schemes based on phase and/or frequency variation. To explore the mechanisms underlying this behavior and their possible functional consequences, we have developed a realistic neural model, based on structural features of visual cortex, which replicates observed oscillatory phenomena. In the model, this oscillatory behavior emerges directly from the structure of the cortical network and the properties of its intrinsic neurons; however, phase coherence is shown to be an average phenomenon seen only when measurements are made over multiple trials. Because average coherence does not ensure synchrony of firing over the course of single stimuli, oscillatory phase may not be a robust strategy for directly encoding stimulus-specific information. Instead, the phase and frequency of cortical oscillations may reflect the coordination of general computational processes within and between cortical areas. Under this interpretation, coherence emerges as a result of horizontal interactions that could be involved in the formation of receptive field properties.

1 Introduction

An obvious characteristic of the general behavior of cerebral cortex, as evident in EEG recordings, is its tendency to oscillate (Bressler and Freeman 1980). Cortical oscillations have been observed both in the electric fields generated by populations of cells (Bressler and Freeman 1980) as well as in the activity of single cells (Llinas 1988). Recent observations of oscillations within visual cortex that are dependent on the nature of the visual stimulus (Gray and Singer 1987; Eckhorn *et al.* 1988; Gray *et al.* 1989; Gray and Singer 1989) have generated increased interest in the role of periodic behavior in cerebral cortical processing in general. These studies have shown that populations of visual cortical neurons at

considerable cortical distances exhibit increased coherence in neuronal activity when the visual stimulus is a single continuous object as compared to a discontinuous object. This work represents an extension of earlier work showing that the responses of cells can be influenced by stimuli that are located beyond of the boundaries of the classical receptive field (Allman *et al.* 1985), with horizontal interactions implicated in shaping these more complex receptive field properties (Tso *et al.* 1986). These recent results have led to suggestions that differences in oscillatory phase and/or frequency between cell populations in primary visual cortex could be used to label different objects in the visual scene for subsequent processing in higher visual areas (Eckhorn *et al.* 1988; Gray *et al.* 1989; Gray and Singer 1989; Sporns *et al.* 1989; Kammen *et al.* 1989). It has further been suggested that these oscillatory patterns may rely on central, extracortical control to assure temporal coherence (Kammen *et al.* 1989).

In this paper we describe the results of simulations of a biologically realistic model of neocortical networks designed to explore the possible mechanisms underlying oscillations in visual cortex, as well as the functional significance of this oscillatory behavior. In particular we analyze the role of horizontal interactions in the establishment of coherent oscillatory behavior.

2 Cortical Model

The model consists of a network of three basic cell types found throughout cerebral cortex (Fig. 1). The principal excitatory neuron, the pyramidal cell, is modeled here as five coupled cylindrical membrane compartments (soma l=20 μm, d=20 μm; dendrites l=100 μm, d=1.5 μm). In addition there are two inhibitory neurons, one principally mediating a slow K^+ inhibition (soma l=10 μm, d=10 μm) and one mediating a fast $C\ell^-$ inhibition (soma l=15 μm, d=15 μm). Both are modeled as a single compartment. Connections between modeled cells are made by axons with finite conduction velocities, but no explicit axonal membrane properties other than delay are included. Synaptic activity is produced by simulating the action-potential triggered release of presynaptic transmitter followed by the activation of the postsynaptic conductance (0.8 msec delay) and the resulting flow of transmembrane current through membrane channels. Each of these channels is described with parameters governing the time course and amplitude of synaptically activated conductance changes. Conductances have single open and closed states with transitions between these states governed by independent time constants. The open time constant for each conductance is 1 msec. The closing time constant for the excitatory conductance is 3 msec, for the $C\ell^-$ inhibitory conductance 7 msec, and for the K^+ inhibitory conductance 100 msec. Each conductance has a driving potential associated with it.

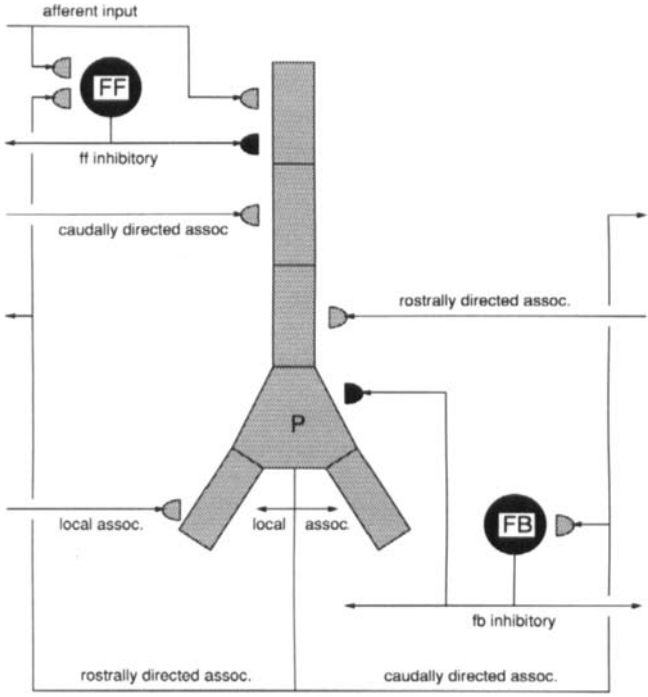

Figure 1: Schematic represention of the local circuit used in the simulations of visual cortex consisting of an excitatory pyramidal cell (P), a feedback inhibitory interneuron (FB), and a feedforward inhibitory interneuron (FF). Darkened half-circles indicate inhibitory synapses; lightened half-circles excitatory synapses.

These potentials are 0 mV for the excitatory conductance, −65 mV for the $C\ell^-$ inhibitory conductance, and −90 mV for the K^+ inhibitory conductance. The compartmental models of the cells integrate the transmembrane and axial currents to produce transmembrane voltages. Basic membrane properties include membrane (r_m = 2000 Ω-cm^2) and axial resistivity (r_a = 50 Ω-cm) and membrane capacitance (c_m = 1 μF/cm^2) with a resting potential of −55 mV (assumed depolarized due to bias of spontaneous input). Excursions of the cell body membrane voltage above a specified threshold (normally distributed: $x = -40$ mV, $\sigma = 2$ mV) trigger action potentials. Following an action potential, there is a 10-msec absolute refractory period during which the cell cannot fire another spike regardless of membrane potential. Additional details of these features of the model are described in Wilson and Bower (1990).

This model is intended to represent a 10×6 mm region of visual cortex. The many millions of actual neurons in this area are represented here by 375 cells (25×15) of the three types for a total of 1125 cells. Input to the model is provided by 100 independent fibers, each making contact within a local cortical region (1 mm^2), and each reflecting the retinotopic organization of many structures in the visual system (Van Essen 1979). The model also includes excitatory horizontal fiber connections between pyramidal cells (Gilbert 1983) (Fig. 1) that extend over a radius of 3 mm from each pyramidal cell (conduction velocity = 0.85 ± 0.13 m/sec; lower bound = 0.45, upper bound = 1.25). Inhibitory cells receive input from pyramidal cells within a 2 mm radius and make connections with pyramidal cells over a radius of 1 mm (Fig. 1) (inhibitory conduction velocity = 1.0 ± 0.06 m/sec; lower bound = 0.8, upper bound = 1.2). The influence of each of these fiber systems falls off exponentially with a space constant of 5 mm. No effort was made to reproduce the periodic structure of actual connections or many other known features of visual cortex. Instead, our intention was to reproduce oscillations characteristic of visual cortex using a small but sufficient set of physiological and anatomical features.

3 Coherent Oscillations

Figure 2 shows auto- and cross-correlations of simulated pyramidal cell spike activity recorded from two sites in visual cortex separated by 6 mm. Total cross-correlations in the modeled data were computed by averaging correlations from 50 individual 500 msec trials. Within each trial, simulated activity was generated by providing input representing bars of light at different locations in the visual field. In these cases, the model produced oscillatory auto- and cross-correlations with peak energy in the 30–60 Hz range, consistent with experimental data (Gray *et al.* 1989). As in the experimental data, the model also produced nearly synchronous oscillatory activity in groups of neurons separated by 6 mm when presented with a continuous bar (Fig. 2A). A broken bar that did not stimulate the region between the recording sites produced a weaker response (Fig. 2B), again consistent with experimental evidence (Gray *et al.* 1989). Shuffling trials with respect to each other prior to calculating cross-correlation functions greatly diminished or completely eliminated oscillations. The same technique applied to actual physiological data yields similar results (Gray and Singer 1989) indicating that while the oscillations are stimulus dependent, they are not stimulus locked. Simulations run in the absence of stimuli produced low baseline activity with no oscillations.

Further analysis of the model's behavior revealed that the 30–60 Hz oscillations are primarily determined by the amplitude and time course of the fast feedback inhibitory input. Increasing the amplitude of the inhibitory input to pyramidal cells reduced oscillatory frequency, while

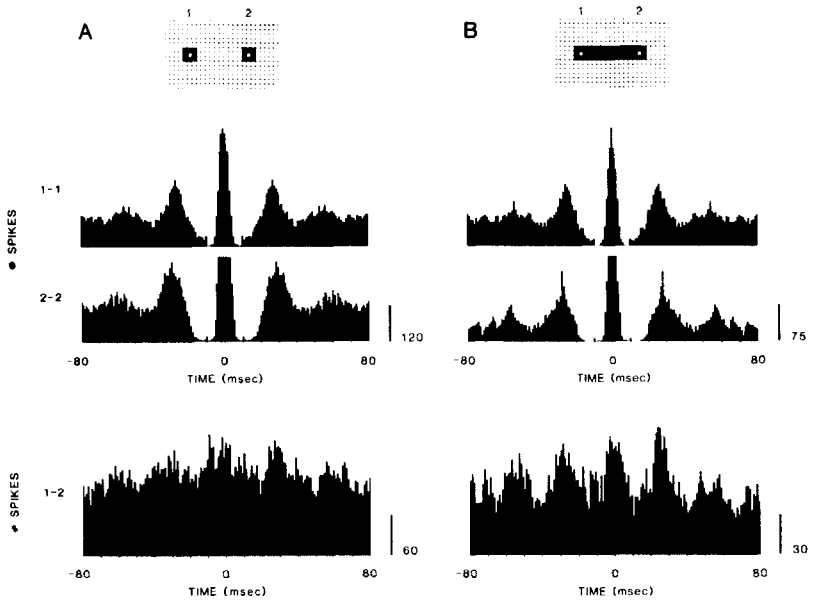

Figure 2: Simulated auto- and cross-correlations generated by presentation of a broken bar (A) and a continuous bar (B) over 500 msec. Upper diagrams show the model with the stimulus region shaded. Grid squares correspond to the location of modeled cells. The numbers indicate the location of the recording sites referred to in the auto- (1–1,2–2) and cross- (1–2) correlations. Methods: Multineuronal activity used to produce the correlations were summed from the 9 neurons nearest each recording site. The stimulus was generated using independent Poisson processes on individual input fibers. The Poisson rate parameter was increased from a baseline of 20 to 500 spikes/sec over the onset period from 20 to 100 msec. The difference in phase between the firing of cells in these locations was estimated by measuring the offset of the dominant peak in the cross-correlation function. These values were consistent with measurements obtained both through chi-square fitting of a modified cosine function and measurement of the phase of the peak frequency component in the correlation function power spectra.

reducing inhibition produced an increase in frequency. Allowing inhibitory cells to inhibit each other within a local region improved frequency locking and produced auto- and cross-correlations with more pronounced oscillatory characteristics.

4 Dependence on Horizontal Interconnections

While the frequency of oscillations was primarily due to local inhibitory circuitry, the coherence in correlated cell firing appears to be related primarily to activity in the horizontal interconnections between pyramidal cells. When all long-range (> 1 mm) horizontal fibers were eliminated, the autocorrelations at each recording site continued to show strong oscillatory behavior, but oscillations in the cross-correlation function vanished (Fig. 3A). Increasing the range of horizontal fibers to 2 mm restored coherent oscillatory behavior (Fig. 3A).

The dependence of phase coherence on horizontal connections immediately raises a number of interesting questions. First, because horizontal fibers have finite conduction velocities, it was surprising that they would produce coherence with zero phase over relatively long distances. If phase coherence was strictly a consequence of horizontal fiber coupling between the recorded cell groups, it seems reasonable to expect a phase difference related to the propagation delay. To explore this further, we reduced the propagation velocity of horizontal fibers from 0.86 ± 0.13 m/sec to 0.43 ± 0.13 m/sec and examined the response to a continuous bar. No effect on phase was found in the cross-correlation function. If, however, the degree of horizontal fiber coupling was enhanced by increasing synaptic weights along horizontal pathways, the cortex displayed a transition from near-zero phase coherence to a phase shift consistent with the delay along the shortest horizontal interconnection path (Fig. 3B).

To examine this result more closely, we analyzed the time course of phase coherence at successive time periods following stimulus onset in both the strong and weakly coupled cases. Initially, in both conditions, the synchronizing effect of the stimulus onset itself produces a tendency for zero-phase correlations during the period from 0 to 125 msec (Fig. 3B). However, in the periods following the onset of the stimulus, when activity is dominated by horizontal fiber effects (125–500 msec), the response differs in the two cases. With enhanced horizontal fiber coupling, nonzero phase shifts emerge that reflect the propagation delays along horizontal fibers (Fig. 3B). However, in the weak coupling case, zero-phase correlations persist, decaying over the entire trial interval (0–500 msec).

5 Mechanisms Governing Coherence

Analysis of the activity patterns generated in the weak coupling condition indicates that the mechanism that sustains the zero-phase bias between distant cell groups after stimulus onset depends on the activation of spatially intermediate cells via horizontal fibers. When this intermediate population of cells is activated by the single stimulus bar, they can activate adjacent cells through their own horizontal fibers in a phase-symmetric fashion. When these intermediate cells are not activated

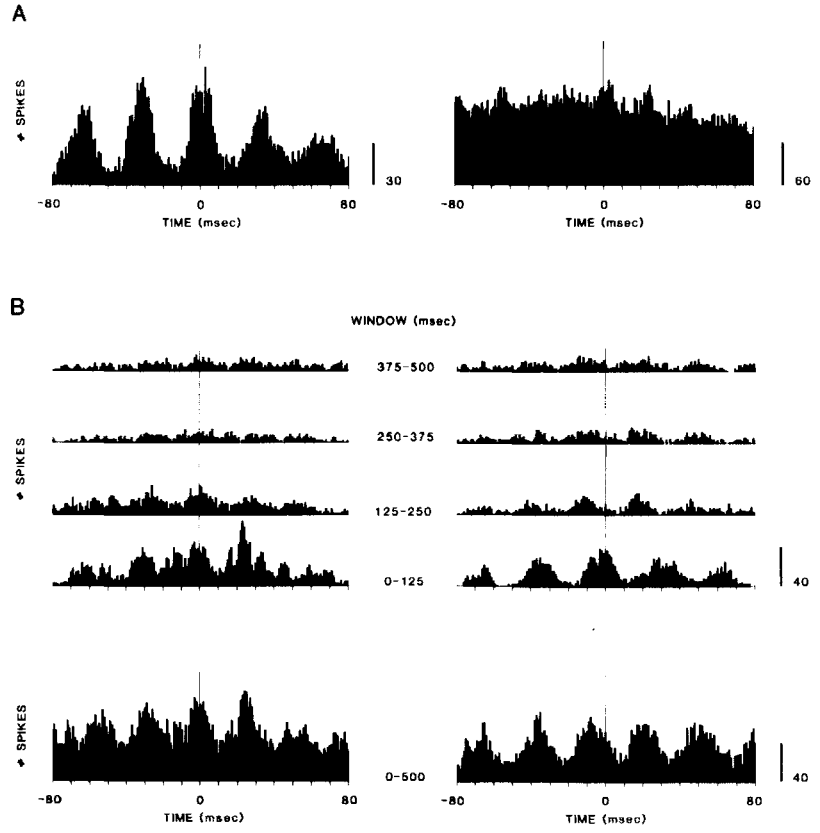

Figure 3: (A) Cross-correlations between sites 1 and 2 (see Fig. 2) for a continuous bar stimulus with radius of horizontal fiber coupling of 2 mm (left) and 1 mm (right). (B) Time course of cross-correlation functions taken at successive 125 intervals over the 500-msec period for relative horizontal fiber coupling strengths of 1 (left) and 1.5 (right). The bottom-most correlation function covers the entire 500-msec interval.

directly by the stimulus, as in the case of the discontinuous bar, their ability to coactivate adjacent cell populations is diminished, resulting in a reduction in observed long-range phase coherence. Increasing the strength of horizontal connections establishes a path of direct polysynaptic coupling between distant sites, which gives rise to systematic phase shifts related to propagation delay.

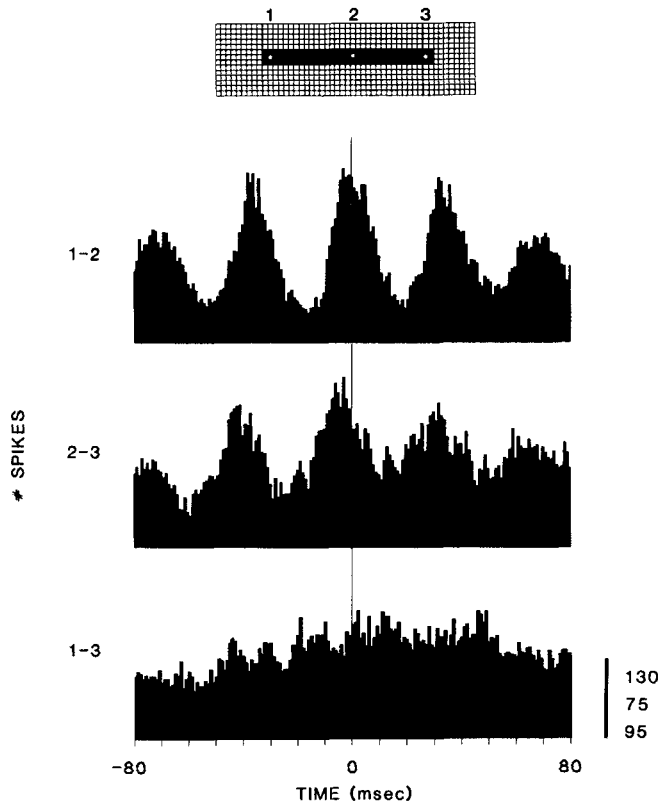

Figure 4: Cross-correlations between sites along a 12-mm stimulus bar.

The model's dependence on horizontal connections for phase coherence leads directly to the prediction that the areal extent of strongest correlations should be related to the spatial spread of the horizontal fibers. This effect was demonstrated in the model by increasing the size of the stimulus bar from 6 to 12 mm in an enlarged cortical simulation in which the horizontal fibers remained at a length of 3 mm. Under these conditions, oscillatory correlations were not found between distant recording sites (1,3 in Fig. 4). Interestingly, correlations were still found between recording points separated by no more than 6 mm (pairs 1,2 and 2,3 in Fig. 4). This absence of transitivity demonstrates the presence of within- and between-trial variations in phase relationships and suggests that the

observed zero-phase phenomena may be present only in the average of multiple trials.

Overall, our simulation results suggest that the oscillatory patterns so far reported to exist in visual cortex can be explained by mechanisms that are entirely intrinsic to the cortical region and do not require an extrinsic driving mechanism (cf. Kammen *et al.* 1989). In the current simulations of visual cortex, we have used long bar stimuli to make the additional prediction that the more restricted extent of horizontal connections should limit coherent correlated activity to an area twice the radius of the horizontal fibers [4–12 mm in cats and monkeys (Gilbert 1983)]. More extensive correlations within primary visual cortex would imply either an additional intrinsic mechanism (e.g., long distance inhibitory coupling) or a more global synchronizing mechanism (Kammen *et al.* 1989). Even if such mechanisms exist, it is likely that they will be coordinated with intrinsic cortical mechanisms.

6 Local Field Potentials

In addition to the observation of synchronized unit activity at spatially separated sites, experimental results also indicate zero-phase synchronization of the oscillatory local field potential (LFP) (Eckhorn *et al.* 1988; Engel *et al.* 1990). Because these potentials are generated principally by dendritic currents summed over large number of cells, LFPs can be evaluated on a trial-by-trial basis. The observation that these potentials are also at zero phase has been taken as evidence for the zero phase relationships between neuronal spiking on individual trials.

In interpreting this observation it must be noted that synchronized LFP is often observed in the absence of unit activity, and that stimulus specificity of synchronized LFP responses differs from unit responses indicating a dissociation of mechanisms giving rise to either phenomena (Gray and Singer 1989; Engel *et al.* 1990).

To understand how synchronized LFP responses could be observed with underlying phase-variable unit responses, it is important to note that LFPs reflect the average input and activity of large numbers of cells. Thus, the presence of adjacent, relatively independent, oscillatory cell groups is sufficient to explain the LFP synchronization in the presence of nonzero instantaneous unit phase relationships, although this has not been directly tested within the model.

For example, two groups of units A and B could show correlated oscillatory behavior with a variable or even consistently nonzero instantaneous phase relationship. If the LFP reflected only the behavior of this population of cells, then the LFP would be expected to reflect the nonzero phase coherence of unit responses. But the presence of additional cell groups, adjacent to but independent of the first group, with

different instantaneous phase relationships would produce a summed contribution to the LFP that would show zero-phase coherence.

Thus, zero-phase as observed in the correlated unit activity may be dependent on trial averaging while zero-phase in the coherence of LFPs may result from spatial averaging of adjacent cell populations with different response properties.

7 Significance of Phase Relationships

Beyond providing a structural explanation for the properties of visual cortical oscillations, our results also have implications for several recently proposed functional interpretations of the observed stimulus-dependent zero-phase coherence. Several researchers have proposed the use of these phase relationships as a means of cortically segmenting, or labeling, different objects in a visual scene (Eckhorn *et al.* 1988; Gray *et al.* 1989; Gray and Singer 1989; Sporns *et al.* 1989; Kammen *et al.* 1989). Associated with this idea, models have been generated that produce the instantaneous phase effects presumably necessary for the visual system to make use of such a coding mechanism on single stimulus trials (Kammen *et al.* 1989). If our results are correct, however, zero-phase relationships between particular neurons should exist, on average, only over multiple trials. The absence of consistent within-trial coherence over long distances would be expected to seriously confound the interpretation of fine phase differences in higher visual processing areas (Wilson and Bower 1990).

Our simulations suggest that the oscillatory behavior seen in visual cortex may be dependent on horizontal interactions that are capable of modulating the responses of widely separated neurons. While the computational function of these types of interactions within the actual cortex is not yet understood, the lateral spread of information could be involved in reinforcing the continuity of visual objects, in modulating classical receptive field properties (Tso *et al.* 1986; Mitcheson and Crick 1982), or in establishing nonclassical receptive field structure (Allman *et al.* 1985). The stimulus dependence of coherence in the model is observed to result from the modulation of the magnitude of these interactions as a function of stimulus structure. Under this interpretation, phase coherence does not in itself encode information necessary for subsequent processing, but rather, phase relationships emerge as a result of the horizontal integration of information involved in the shaping of receptive field properties.

8 General Cerebral Cortical Processing

For the last several years we have been using biologically realistic computer simulations to study the oscillatory behavior of another primary sensory region of cerebral cortex, the olfactory or piriform cortex (Wilson and Bower 1988, 1989, 1990, 1992). This structure is also known to

generate oscillatory activity in the 40 Hz range under a variety of experimental conditions (Adrian 1942; Freeman 1968, 1978). It is interesting to note that the neural mechanisms that generate the oscillatory behavior described here in the visual cortex model are also capable of reproducing the basic frequency and phase relationships of olfactory cortex. In each case inhibitory neurons govern the frequency of the oscillations while the long-range horizontal connections are involved in establishing specific phase relationships. Our work in piriform cortex suggests that the 40 Hz cycle reflects a fundamental cortical processing interval while phase relationships, as in the model of visual cortex, reflect the structure of intercellular communication within the network (Wilson and Bower 1992). If true, then this 40 Hz oscillatory structure may reflect very general properties of cerebral cortical function.

Acknowledgments

This research was supported by the NSF (EET-8700064), the ONR (N00014-88-K-0513), and the Lockheed Corporation. We wish to thank Christof Koch and Dan Kammen for valuable discussions.

References

Adrian, E. D. 1942. Olfactory reactions in the brain of the hedgehog. *J. Physiol. (London)* **100**, 459–472.

Allman, J., Miezin, F., and McGuinness, E. 1985. Stimulus specific responses from beyond the classical receptive field: Neurophysiological mechanisms for local-global comparisons in visual neurons. *Ann. Rev. Neurosci.* **8**, 407–430.

Bressler, S. L., and Freeman, W. J. 1980. Frequency analysis of olfactory system EEG in cat, rabbit and rat. *Electroenceph. Clin. Neurophysiol.* **50**, 19–24.

Eckhorn, R., Bauer, R., Jordan, W., Brosch, M., Kruse, W., Munk, M., and Reitboeck, H. J. 1988. Coherent oscillations: A mechanism of feature linking in the visual cortex? *Biol. Cybern.* **60**, 121–130.

Freeman, W. J. 1968. Relations between unit activity and evoked potentials in prepyriform cortex of cats. *J. Neurophysiol.* **31**, 337–348.

Freeman, W. J. 1978. Spatial properties of an EEG event in the olfactory bulb and cortex. *Electroenceph. Clin. Neurophysiol.* **44**, 586–605.

Gilbert, C. D. 1983. Microcircuitry of the visual cortex. *Ann. Rev. Neurosci.* **6**, 217–247.

Gray, C. M., and W. Singer. 1987. Stimulus-specific neuronal oscillations in the cat visual cortex: A cortical functional unit. *Soc. Neurosci. Abstr.* **404**, 3.

Gray, C. M., and Singer, W. 1989. Stimulus specific neuronal oscillations in orientation columns of cat visual cortex. *Proc. Natl. Acad. Sci. U.S.A.* **86**, 1698–1702.

Gray, C. M., Konig, P., Engel, A. K., and Singer, W. 1989. Oscillatory responses in cat visual cortex exhibit inter-columnar synchronization which reflects global stimulus properties. *Nature (London)* **338**, 334–337.

Kammen, D. M., Holmes, P. J., and Koch, C. 1989. Cortical architecture and oscillations in neuronal networks: Feedback versus local coupling. In *Models of Brain Function*, R. M. J. Cotterill, ed. Cambridge Univ. Press, Cambridge.

Llinas, R. 1988. The intrinsic electrophysiological properties of mammalian neurons: Insights into central nervous system function. *Science* **242**, 1654–1664.

Mitchison, G., and Crick, F. 1982. Long axons within the striate cortex: Their distribution, orientation and patterns of connection. *Proc. Natl. Acad. Sci. U.S.A.* **79**, 3661–3665.

Sporns, O., Gally, J. A., Reeke, G. N., Jr., and Edelman, G. M. 1989. Reentrant signaling simulated neuronal groups leads to coherency in their oscillatory activity. *Proc. Natl. Acad. Sci. U.S.A.* **86**, 7265–7269.

Tso, D. Y., Gilbert, C. D., and Wiesel, T. N. 1986. Relationships between horizontal interactions and functional architecture in cat striate cortex as revealed by cross-correlation analysis. *J. Neurosci.* **6**, 1160–1170.

Van Essen, D. C. 1979. Visual areas of the mammalian cerebral cortex. *Ann. Rev. Neurosci.* **2**, 227–263.

Wilson, M. A., and Bower, J. M. 1988. A computer simulation of olfactory cortex with functional implications for storage and retrieval of olfactory information. In *Neural Information Processing Systems*, D. Z. Anderson, ed. AIP Press, New York.

Wilson, M. A., and Bower, J. M. 1989. The simulation of large scale neuronal networks. In *Methods in Neuronal Modeling: From Synapses to Networks*, C. Koch and I. Segev, eds., pp. 291–334. MIT Press, Cambridge, MA.

Wilson, M. A., and Bower, J. M. 1990. Computer simulation of oscillatory behavior in cerebral cortical networks. In *Advances in Neural Information Processing Systems*, Vol. 2, D. Touretzky, ed., pp. 84–91. Morgan Kaufmann, San Mateo, CA.

Wilson, M. A., and Bower, J. M. 1992. Cortical oscillations and temporal interactions in a computer simulation of piriform cortex. *J. Neurophysiol.*, in press.

Received 23 July 1990; accepted 5 June 1991.